# An Empirical Modelling for the Baseline Energy Consumption of an NB-IoT Radio Transceiver

Sikandar Zulqarnain Khan*, Muhammad Mahtab Alam *, Yannick Le Moullec*, Alar Kuusik*,
Sven Pärand**, Christos Verikoukis ***
*Thomas Johann Seebeck Department of Electronics, Tallinn University of Technology, Tallinn, Estonia,
**Telia Estonia, *** Centre Tecnològic de Telecomunicacions de Catalunya (CTTC)
sikandar.khan, muhammad.alam, yannick.lemoullec, alar.kuusik@taltech.ee,
svend.parand@telia.ee, cveri@cttc.es

***Abstract*—NarrowBand Internet of Things (NB-IoT) is an emerging cellular IoT technology that offers attractive features for deploying low-power wide area networks suitable for implementing massive machine type communications. NB-IoT features include e.g. extended coverage and deep penetration for massive connectivity, longer battery-life, appropriate throughput and desired latency at lower bandwidth. Regarding the device energy consumption, NB-IoT is mostly under-estimated for its control and signaling overheads, which calls for a better understanding of the energy consumption profiling of an NB-IoT radio transceiver. With this aim, this work presents a thorough investigation of the energy consumption profiling of Radio Resource Control (RRC) communication protocol between an NB-IoT radio transceiver and a cellular base-station. Using two different commercial off the shelf NB-IoT boards and two Mobile Network Operators (MNOs) NB-IoT test networks operational at Tallinn University of Technology, Estonia, we propose an empirical baseline energy consumption model. Based on comprehensive analyses of the profile traces from the widely used BG96 NB-IoT module operating in various states of RRC protocol, our results indicate that the proposed model accurately depicts the baseline energy consumption of an NB-IoT radio transceiver while operating at different coverage class levels. The evaluation errors for our proposed model vary between 0.33% and 15.38%.**

***Index Terms*—LPWAN, NB-IoT, Empirical Energy Consumption Model, Power consumption, NB-IoT networks, BG96 chip.**

## I. INTRODUCTION

The third generation partnership project (3GPP) has introduced two new cellular technologies to enable a wide range of cellular communications specifically for machine-to-machine and Internet of Things applications. These include LTE-M (Long Term Evolution for Machines) and NB-IoT (NarrowBand-IoT) technologies. On the one hand, LTE-M includes LC-LTE/MTCe (LTE Cat 0) and eMTC (enhanced Machine Type Communication) technologies (wherein eMTC includes LTE Cat M1 and LTE Cat M2), particularly targeted at applications that require mobility and higher data rates [1]. On the other hand, NB-IoT includes LTE CAT-NB1 and LTE CAT-NB2 technologies, particularly targeted at applications that require lower complexity and lower data rates [2]. Furthermore, both eMTC and NB-IoT are built upon the existing and already deployed 4G LTE infrastructure to support energy-constrained, mostly battery-powered IoT devices.

To reduce the power consumption of an end-device, also called a User Equipment (UE), both eMTC and NB-IoT provide extended versions of the existing power saving features of the legacy LTE technology i.e., eXtended Discontinuous Reception (eDRX) and Power Saving Mode (PSM) to help prolong the UE's battery lifetime [3], [4]. Utilizing these features in the UE requires a Radio Resource Control (RRC) connection setup between the UE and the network; a detailed overview of this RRC protocol is provided in Section II of this paper.

The eDRX feature enables the device to switch off parts of its radio circuitry, thereby operating with limited functionality and thus reduced power consumption [5], making it a useful feature for network-oriented applications where the device can be woken up remotely by the network as needed, e.g., in smart-grid applications. The PSM feature, on the other hand, enables the device to switch off its radio circuity, thereby operating with lowest possible power consumption [5], making it a useful feature for device-oriented applications where the device is not accessible to the network but is woken up locally as scheduled (time-triggered) by the application e.g., in smart-metering and public-bike-sharing applications etc.

A typical NB-IoT device include a radio transceiver, a microcontroller, and additional peripherals as its main components; among them, the radio transceiver has significantly higher energy consumption. Thus, understanding the details of the energy consumption of the radio transceiver is an important research topic in order to better estimate the lifetime of NB-IoT devices.

### A. State of the art

Several works have evaluated NB-IoT technology in terms of its UE's power consumption analysis and battery life-time estimations [6-22] that can be categorized into analytical, simulations, and experimental measurements based analysis. Most of these works provide analytical models with simulation based energy estimations [6]–[14]. For example, the work in [6] focus on finding the optimum length of an eDRX cycle to help mitigate the signaling cost in an LTE network with simulations based analysis. The authors in [8] have presented an NB-IoT energy consumption model with

uplink and downlink data transmissions as defined by Poisson processes. The authors in [9] and [10] have tried to estimate the NB-IoT device battery life-time by using some simplified energy consumption equations, whereas the authors in [12] have proposed an NB-IoT UE energy consumption analytical model based on Markov chains. Similarly, the work in [14] presents an analytical model for evaluating the latency and maximum number of devices in any network. Overall, most of the analytical models as presented in these works have been validated through network simulators. Such validations have higher uncertainty as the models estimates and the validation errors do not use accurate actual measurements.

Several works have also provided experimental power consumption analysis of the NB-IoT technology, such as [15]–[22]. For example, the work in [15] focuses on the design of an NB-IoT prototype for delay-tolerant applications while operating in different coverage levels of the network. Although this work provides power consumption measurements of the NB-IoT UE as a whole, the individual power consumption details for each state of the operating mode of radio/node are missing. The work in [16] focuses on the latency issues of NB-IoT while making use of a commercial NB-IoT network in Belgium. Although this work provides empirical results for analyzing the network performance in terms of setup times, throughput, and latency, it does not present the power consumption details of the UE. The work in [17] provides empirical results for the current traces of CoTS NB-IoT platform i.e., Ublox SARA-N211 while operating on Vodafone's network in Barcelona, Spain. While this work provides coarse-grained current traces for the various states of the radio i.e., C-DRX, I-DRX, and PSM; the underneath fine-grained details for their respective C-DRX cycles, eDRX cycles and their PTWs, I-DRX cycles with SPs and POs are missing.

The authors in [19] claim to provide the first publicly available empirical power consumption measurements for the NB-IoT devices but their measurement setup is emulated using a Keysight UXM, a standard-compliant NB-IoT BS emulator; so, it is unclear to what extent their results would map onto a real network. Similarly, the work in [21] proposes a Dual-RAT LPWAN node combining an NB-IoT and LoRaWAN radio into one node with all the necessary power regulator circuitry. Here too, the power consumption numbers for the whole node are given where the individual power graphs for each radio and their internal state details are missing.

Considering the above sate-of-the-art and to the best of our knowledge, the following research gaps exist in the literature. First, no detailed baseline power consumption assessment of the NB-IoT radio has yet been provided in the literature. Second, an accurate energy consumption model that truly depicts the empirical energy consumption of an NB-IoT radio across its various stages of RRC operation (i.e., attach, active waiting, idle waiting, resume) is missing. Third, recently published works on the NB-IoT UE's power consumption present only a coarse-grain analysis of the NB-IoT node(s), providing mostly the aggregated power consumption details of the whole node where the individual power consumption details of the underneath activities remain mostly obscured. That is why the detailed energy-consumption profiling of the various states of the CoTS NB-IoT radio module(s) and its underneath activities remain unexplored to date. Fourth, most of the existing analyses are based on emulated NB-IoT networks (in particular the base-station (BS)) and not on actual network operating BS. Similarly, the detailed energy consumption profiling of the commercially available (CoTS) NB-IoT devices under real mobile network operators (MNOs) networks are yet to be explored.

### *B. Contributions*

This work provides a modelling methodology for profiling the baseline energy consumption of an NB-IoT radio transceiver based on its detailed empirical measurements. The modelling methodology exploits all the states of the RRC protocol standardized by 3GPP and hence is applicable to general NB-IoT radio chips that are standard compliant.

The main contributions of our paper and positioning with reference to the state of the art can be summarized as follows:

• Decomposing of the LTE RRC protocol with precise details and experimental demonstrations: while the 3GPP standard documentation ( [4], [23]–[25]) and a number of papers in the literature (among others [17]) present the key concepts of the LTE RRC protocol, to the best of our knowledge, this work is the first one to delve into a fine grain analysis of the LTE RRC protocol while mapping its different stages and modes with equally detailed experimental results in terms of energy consumption, thereby providing details and a level of understanding of the baseline energy consumption not available so far.

• Empirical and detailed power consumption measurements of CoTS NB-IoT radio transceiver while operating under real networks: in contrast to most existing works (e.g., [17], [19], [21]) that are limited to the aggregated power or energy consumption of the whole NB-IOT UE and/or rely on either simulations or emulated networks, this work analyzes the energy consumption of the radio transceiver in details (i.e. for each state of the RRC protocol) while operating under two MNOs deployed NB-IoT test networks; this provides not only a more detailed analysis but also more realistic empirical-based results as compared to the state of the art.

• Derivation of an accurate energy consumption model for an NB-IoT radio transceiver: existing models are analytical only and/or not detailed enough to reflect all the inner mechanisms at play in the NB-IoT radio. To overcome this gap, and to the best of our knowledge, we are the first ones to propose a detailed and realistic NB-IoT radio transceiver energy consumption model thanks to the detailed analysis and real-life empirical experiments mentioned above.

• The proposed model is evaluated under real life conditions, we calculated the difference between the energy consumption obtained from the real life deployment versus the energy consumption predicted by using our proposed model. Our results show that the error of the proposed model ranges

between 0.33% and 15.38%, mostly incurring deviation in the attach and resume procedures.

The remainder of this paper is organized as follows. Section II provides an overview of the RRC protocol whereas Section III presents our proposed NBIoT radio energy consumption model. Section IV presents the empirical measurement results of the NB-IoT radio energy consumption at its various states of operation where Section V presents the evaluation of the proposed model. Section VI sums up our conclusions and future works.

## II. Overview of Radio Resource Control (RRC) Protocol

The RRC is a communication protocol between an end device/UE and the base-station (also termed evolved Node-B (eNB)) through which network services such as connection establishment, connection maintenance, data exchange, sleep and notification patterns, security and Quality of Service (QoS), etc. take place. The RRC protocol model has only two complementary states i.e., 1) RRC_Connected and 2) RRC_Idle as shown in the RRC protocol reference model in Figure 1 such that the radio alternates between these two states during its operation.

As shown in Figure 1, the UE, on power up (or cold start), requests a network connection from the base-station which upon acknowledgement is granted network resources and it thus enters into the RRC_Connected state. The connection establishment happens in the "Attach" procedure and is always initiated by the UE. Once connected, the exchange of uplink(Tx)/downlink(Rx) data between the UE and the network takes place in the allocated transmission and reception slots that have been previously allocated to the UE during the Attach process. After a secure exchange of data, the UE listens to the broadcast information from the eNB for a certain period of time that is termed "Active waiting" and whose period is set by the network operator. If downlink data from the eNB is monitored during this period, the RRC connection is resumed so that the exchange of data between the network and UE occurs; at the end of the last data transmission the active waiting period restarts from zero. If no data arrives during Active waiting, the eNB releases the connection and the UE switches to RRC_Idle state, thereby saving all the context of the network in local memory.

Transiting into RRC_Idle state, the UE may enter either into eXtended Discontinuous Reception mode (eDRX) or into Power Saving Mode (PSM) as per its configuration. The UE can also alternate between these two states, with eDRX first and PSM next, if both states are enabled. In the eDRX mode, the UE listens to the broadcast information from the eNB in cyclic patterns known as eDRX cycles; hence this phase is termed as eDRX mode. During the eDRX mode, the UE listens to the broadcast information from the network in pre-defined slots, thus with limited functionality, that results in reduced energy consumption of the radio. When the eDRX mode expires, or when it is forced to expire, the UE switches to the PSM mode during which it turns off its radio and is therefore not reachable by the network. This mechanism facilitates the device to enter deeper hardware sleep modes and thus contribute towards maximum power savings of the UE's battery, but at the cost of increased latency.

To summarize, the NB-IoT radio goes through the following states as it operates under the RRC protocol i.e., (i) Attach – registration to the network on a cold start or power up, (ii) Data Exchange (Tx/Rx) – transmission and reception of data to/from the network, (iii) Active Waiting (C-DRX mode) - continuous listen to the broadcast information from the eNB for a period as permitted by the network operator and as configured by the UE, (iv) Idle Waiting (eDRX mode) – partly listens to the broadcast information from eNB for a period as permitted by the operator and as configured by the UE, (vi) Power Saving Mode (PSM) - shut-down of the radio activity for a period as requested by the UE and that as acknowledged by the network, and (viii) Tracking Area Update (TAU) - Resuming the connection with eNB on wake up from PSM. All these radio states are shown in the RRC reference model in Figure 1. Details of these radio states are discussed in what follows.

### A. Attach - RRC_Connected state

On powering up, the radio scans the air for a suitable network interface through a contention-based Random Access (RA) preamble to which the eNB responds with a Random Access Response (RAR) message. The UE then sends an RRC connection request to which the eNB responds with an RRC connection setup and the UE thus gets connected to the eNB. Afterwards, the UE establishes a connection with the core network and generates an Access Stratum (AS) security context for secure exchange of data. After a successful AS security setup, the eNB reconfigures the RRC connection to finally establish a data radio bearer for the UE to uplink its data packets in the allocated transmission (Tx) slots. Further details on the attach procedure can be found in [24] and [25].

### B. Data Exchange (Tx/Rx) - RRC_Connected state

When the UE wants to transmit some data to the network, it first establishes an RRC connection with the network through an Attach procedure (on powering up) or TAU procedure (on waking up from PSM) and transits to the RRC Connected state. It then transmits its data packets to the network in its allocated transmission (Tx) slots using some transmission protocols (such as UDP, HTTPS, MQTT etc). On the other hand, when the network wants to transmit some data to the UE (i.e., the UE will now receive data), there are two possibilities for the network to reach the UE in its RRC_Idle state, depending on whether it is in eDRX or PSM mode. If the UE is in eDRX mode, it periodically listens to the broadcast messages from the network during the paging occasions (PO) of each I-DRX cycle. In this case, the network sends a paging message to the UE and notifies it of the pending downlink traffic. As the UE interprets the paging message, it initiates a connection resume/reconnect procedure to get connected to the network and thus the exchange of downlink data between

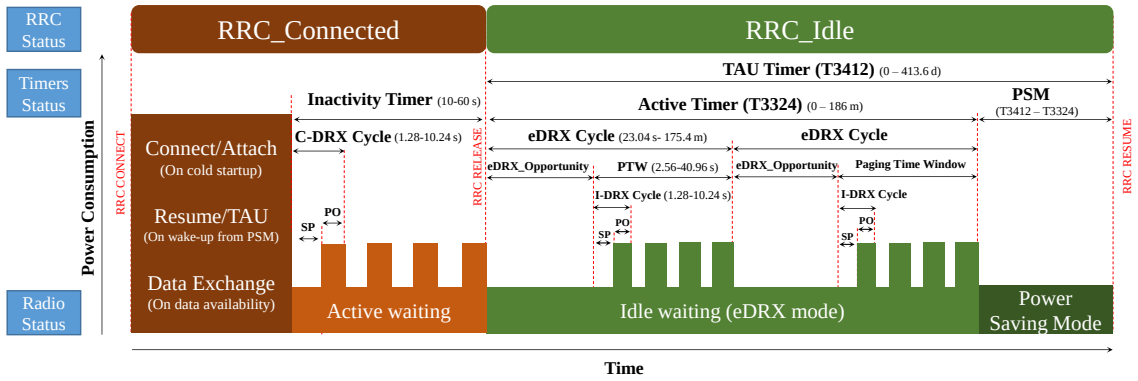


Figure 1: RRC protocol reference model for the NB-IoT radio that is composed of two complementary states i.e., RRC_Connected and RRC_Idle; exploiting Active waiting, Idle waiting and Power Saving Mode (PSM) after connection establishment with the network. From top to bottom: (top) RRC connection status, (middle) involved timers with their minimum and maximum limits and (bottom) radio status with associated power consumption as depicted schematically.

the UE and network occurs in the allocated reception (Rx) slots. However, if the UE is in PSM mode, it is not reachable by the network until the expiration of its PSM period (i.e., T3412-T3324). As the PSM expires, the UE initiates the TAU procedure to resume connection with the network after which the data exchange occur. More details on data exchange can be found in [11] and [26].

### C. Active waiting - RRC_Connected state

Discontinuous Reception (DRX) is a legacy LTE feature that enables the UE to discontinuously receive the Physical Downlink Control Channel (PDCCH) to maintain network synchronization and determine if there is any pending downlink data. The DRX feature can be enabled both in the RRC_Connected state, i.e., Connected-DRX (C-DRX), and in the RRC_Idle state, i.e., Idle-DRX (I-DRX) in the LTE RRC protocol. In the RRC_Connected state, when there is no data traffic, the UE alternates between a Sleep Period (SP) during which the radio remains quiet and a Paging Occasion (PO), also called Paging Event (PE), during which the radio monitors the PDCCH such that SP and PO alternates in a cyclic pattern that is termed as C-DRX cycle (C for connected state of the radio). These patterns of SPs and POs (i.e., C-DRX cycles) repeat for the entire duration of Active waiting whose length is controlled by the value of the Inactivity Timer. The value of the Inactivity Timer is operator specific and is 10-60 s in most commercial network. However, it is upto the network operator to set its duration. Secondly, the UE can only control it to the extent the operator permits and it cannot impose its configuration over the operator allowed limits. Furthermore, the Inactivity Timer starts running automatically at the end of the last transmission of data where upon its expiration the network releases the connection and the device switches to RRC_Idle state [23]. If some data arrives while the UE is still in its active waiting phase, the connection is resumed for the exchange of data between the UE and the network in the allocated data exchange slots; where the Inactivity Timer restarts and the UE thus enters into its active waiting once again.

### D. Idle waiting (eDRX mode) - RRC_Idle state

In the RRC_Idle state, new resources cannot be requested from the network. However, the UE is still reachable by the network where it periodically monitors the Physical Downlink Control Channel (PDCCH) in cyclic patterns. The NPDCCH monitoring takes place during the on-phase of an I-DRX cycle (I for Idle state of the radio), i.e., PO or PE where during the next off-phase of the I-DRX cycle i.e., SP, the radio does not perform any activity. These I-DRX cycles repeat for the entire duration of a "Paging Time Window (PTW)"; where PTW itself forms the active phase of an eDRX Cycle; such that each PTW is followed by an inactive phase that is termed as eDRX_Opportunity where the radio remains quiet until the beginning of the next PTW. These cyclic patterns of eDRX_Opportunity and PTW i.e, eDRX Cycle occur repeatedly during the entire span of the Idle waiting state of the radio. And since Idle waiting involves repeated eDRX cycles, this phase is also termed as eDRX mode. All these nested cycles of activity and inactivity during the eDRX mode are shown in the RRC protocol reference model in Figure 1.

The eDRX mode is controlled by a set of timers where the active timer (i.e., T3324) primarily controls the time lapse of the entire duration of the eDRX mode and can have an extended range from 0-186 m for NB-IoT, with a maximum period of 175.4 m for its eDRX cycle and a maximum period of 40.96 s for its PTW. Similarly, the maximum I-DRX cycle can be of 10.24 s for NB-IoT. The minimum and max limits of these cycles for NB-IoT technology are also indicated in the RRC protocol reference model in Figure 1. Further details on their minimum and maximum ranges can be found in [4], [5]. It is worth mentioning here that the UE can configure the length of its eDRX mode, the length of its eDRX cycle, and the duration of its PTW, only if permitted by the network.

### E. PSM - RRC_Idle state

On expiration of the active (T3324) timer, the UE exits Idle waiting (eDRX mode) and enters into the Power Saving Mode (PSM). While in PSM, the UE turns its radio off for as long as the TAU timer is running and its energy consumption approaches to almost its power-off state. It is worth noting that though the radio or UE is not reachable by the network, it is still registered with the network so that when the UE wakes-up from its PSM, it does not have to go through the registration process once again, saving a significant amount of signaling overhead. Further details on the resume procedure can be found in [24], [25] and [13], [26].

As the TAU (T3412) timer expires, the PSM is exited and the UE wakes up to perform the Tracking Area Update (TAU) where the already registered UE reconnects with the network to check whether there is any pending uplink/downlink data. Once this data exchange has occurred, the period of active waiting starts where upon its end the UE enters into the RRC_Idle state and the cycle repeats. It should be noted here that the PSM mechanism implies a low power consumption at the cost of higher latency because the network has to wait until the UE is up again from the PSM and reachable by the network. As NB-IoT is designed for latency-tolerant applications, the UE may (deep) sleep for an extended range of 413 days and still be registered with the network. More details on the PSM state can be found in [4], [17].

### F. Tracking Area Update (TAU) - RRC_Connected state

On expiration of the TAU (T3412) timer, the device wakes-up from PSM and reconnects to indicate to the network its availability in the tracking area update (TAU) procedure. During the TAU procedure, the UE listens to any scheduled DL data that if exists is downloaded in the allocated reception (Rx) slots. Similarly, if the UE has any UL data, it is transferred to the network in the allocated transmission (Tx) slots. If no data exists for exchange, the Inactivity timer starts so that the device enters into Active waiting. As it finishes, the device enters into Idle waiting and the cycle continues. Further details on the TAU procedure can be found in [4], [24], [25].

This section has presented an in-depth analysis of the NB-IoT RRC protocol phases; thanks to this knowledge, we can now proceed with building a mathematical and empirical NB-IoT UE energy consumption model, which we describe in the next sections.

## III. Proposed Model for Profiling the Baseline Energy Consumption of NB-IoT Radio Transceiver

In addition to the detailed analysis of the RRC protocol presented in the previous section, a mathematical model that provides a detailed baseline energy consumption of the RRC protocol is presented in this section.

Since the RRC protocol has only two states, i.e., 1) RRC_Connected and 2) RRC_Idle, the total energy consumed by an RRC radio can be given as:

$$E_{TOTAL} = E_{RRC\_CONNECTED} + E_{RRC\_IDLE} \quad (1)$$

In the RRC_Connected state, the radio goes through the four following states i.e., Attach, Data Exchange (Tx/Rx), Active waiting and TAU such that the Attach procedure occurs only after a cold start whereas the TAU procedure occurs each time the radio wakes up from its PSM. Thus the total energy consumed during the RRC_Connected state can be written as:

$$\begin{aligned} E_{RRC\_CONNECTED} = E_{ATTACH} + E_{Tx/Rx} \\ + E_{ActiveWaiting} + E_{TAU} \end{aligned} \quad (2)$$

As the Inactivity Timer finishes, the RRC connection is released and the radio goes into RRC_Idle state where the radio first enters into Idle waiting state or eDRX mode followed by PSM state. Thus the total energy consumed during the RRC_Idle state can be written as:

$$E_{RRC\_IDLE} = E_{eDRX} + E_{PSM} \quad (3)$$

Since $Energy = Power \times Time$; the average energy consumption during the RRC_Connected state can be written as:

$$\begin{aligned} E_{RRC\_CONNECTED} = \\ \{P_{ATTACH(avg)} \times T_{ATTACH}\} + \{(P_{Tx(avg)} \times T_{Tx}) \\ + (P_{Rx(avg)} \times T_{Rx})\} + \{P_{ActiveWaiting(avg)} \\ \times T_{InactivityTimer}\} + \{P_{TAU(avg)} \times T_{T3412}\} \end{aligned} \quad (4)$$

Since $ActiveWaiting$ period is a series of repeated C-DRX cycles, the above equation can be written as:

$$\begin{aligned} E_{RRC\_CONNECTED} = \{P_{ATTACH(avg)} \times T_{ATTACH}\} + \\ \{(P_{Tx(avg)} \times T_{Tx}) + (P_{Rx(avg)} \times T_{Rx})\} + \{P_{ActiveWaiting(avg)} \\ \times (T_{CDRX\_Cycle} \times N_{CDRX\_Cycles})\} + \{P_{TAU(avg)} \times T_{TAU}\} \end{aligned} \quad (5)$$

where $T_{CDRX\_Cycle}$ is the time period of each C-DRX cycle and $N_{CDRX\_Cycle}$ are the total number of C-DRX cycles that occur during the $ActiveWaiting$ period.

Similarly, the average energy consumption of the radio during the RRC_Idle state is:

$$E_{RRC\_IDLE} = E_{eDRX} + E_{PSM} \quad (6)$$

In terms of power calculations, the above equation becomes:

$$\begin{aligned} E_{RRC\_IDLE} = \\ \{P_{eDRX(avg)} \times T_{eDRX}\} + \{(P_{PSM(avg)} \times T_{PSM}\} \end{aligned} \quad (7)$$

The duration of the entire Idle state of the radio, its eDRX mode and PSM can be set by the values of 3GPP specified timers, such that:

$$T_{RRC\_IDLE} = T_{3412} \quad (8)$$

$$T_{eDRX} = T_{3324} \quad (9)$$

$$T_{PSM} = T_{3412} - T_{3324} \quad (10)$$

Thus the above equation can be written as:

$$\begin{aligned} E_{RRC\_IDLE} = \{P_{eDRX(avg)} \times T_{3324}\} \\ + \{P_{PSM(avg)} \times (T_{3412} - T_{3324})\} \end{aligned} \quad (11)$$

Since the $eDRX$ mode is composed of repeated $eDRX$ cycles, thus:

$$E_{RRC\_IDLE} = \{P_{eDRX(avg)} \times (T_{eDRX\_Cycle} \times N_{eDRX\_Cycles})\} + \{(P_{PSM(avg)} \times (T_{3412} - T_{3324})\} \quad (12)$$

where $T_{eDRX\_Cycle}$ is the time period of each eDRX cycle and $N_{eDRX\_Cycles}$ are the total number of eDRX cycles that occur during the $IdleWaiting$ period.

Since each $eDRXcycle$ is composed of a $PTW$ (active phase of an $eDRXcycle$) and $eDRX\_opportunity$ ( inactive phase of an $eDRXcycle$), the above equation can be extended to:

$$E_{RRC\_IDLE} = \{P_{eDRX(avg)} \times (T_{eDRX\_PTW} + T_{eDRX\_OPP}) \times N_{eDRX\_Cycles}\} + \{(P_{PSM(avg)} \times (T_{3412} - T_{3324})\} \quad (13)$$

Since the power consumption of $PTW$ and $eDRX\_opportunity$ during each $eDRXcycle$ is different, the above equation can be written as:

$$E_{RRC\_IDLE} = \{(P_{eDRX\_PTW(avg)} \times T_{eDRX\_PTW}) + (P_{eDRX\_OPP(avg)} \times T_{eDRX\_OPP}) \times N_{eDRX\_Cycles}\} + \{(P_{PSM(avg)} \times (T_{3412} - T_{3324})\} \quad (14)$$

As $PTW$ is repeated sequence of $I - DRX$ cycles. Thus:

$$E_{RRC\_IDLE} = \{(P_{eDRX\_PTW(avg)} \times (T_{I-DRX\_Cycle} \times N_{I-DRX\_Cycles}) + (P_{eDRX\_OPP(avg)} \times T_{eDRX\_OPP}) \times N_{eDRX\_Cycles}\} + \{(P_{PSM(avg)} \times (T_{3412} - T_{3324})\} \quad (15)$$

where $T_{I-DRX\_Cycle}$ is the time period of each $I - DRX$ cycle and $N_{I-DRX\_Cycles}$ are the total number of $I - DRX$ cycles occurring during the $PTW$ of each $eDRXcycle$.

Since, each $I - DRX$ cycle has an on phase (PO) during which the NPDSCCH signal is monitored and an off phase of no activity. Thus the above equation can be extended to:

$$E_{RRC\_IDLE} = \{(P_{I-DRX\_on(avg)} * T_{I-DRX\_on}) + (P_{I-DRX\_off(avg)} \times T_{I-DRX\_off}) \times N_{I-DRX\_Cycles}) + (P_{eDRX\_OPP(avg)} \times T_{eDRX\_OPP}) \times N_{eDRX\_Cycles}\} + \{(P_{PSM(avg)} \times (T_{3412} - T_{3324})\} \quad (16)$$

Finally:

$$E_{TOTAL} = E_{RRC\_CONNECTED} + E_{RRC\_RELEASED} \quad (17)$$

thus,

$$E_{TOTAL} = \Big\{\{P_{ATTACH(avg)ATTACH}\} + \{(P_{Tx(avg)Tx}) + (P_{Rx(avg)Rx})\} + \{P_{ActiveWaiting(avg)} \times (T_{CDRX\_Cycle\ CDRX\_Cycles})\} + \{P_{TAU(avg)} \times T_{TAU}\}\Big\} + \Big\{\{(P_{I-DRX_{on(avg)}I-DRX_{on}}) + (P_{I-DRX_{off(avg)}} \times T_{I-DRX_{off}}) \times N_{I-DRX\_Cycles}\} + \{(P_{eDRX\_OPP(avg)}T_{eDRX\_OPP)}\ _{eDRX\_Cycles}\} + \{P_{PSM(avg)} \times (T_{3412} - T_{3324})\}\Big\} \quad (18)$$

For simplicity, the above equation can be rearranged in terms of the 3GPP specified timers such that each row in the following equation represents the energy consumption of each separate state of the radio i.e, Attach, Data Exchange, Active waiting, light sleep (eDRX), deep sleep (PSM) and TAU, i.e.,

$$E_{TOTAL} = \begin{pmatrix} \{P_{ATTACH(avg)} \times T_{ATTACH}\} + \\ \{(P_{Tx(avg)}T_{Tx}) + (P_{Rx(avg)}T_{Rx})\} + \\ \{P_{ActiveWaiting(avg)}(T_{InactivityTimer})\} + \\ \{P_{TAU(avg)} \times T_{3412}\} \end{pmatrix} + \begin{pmatrix} \{(P_{eDRX(avg)} \times T_{3324})\} + \\ \{P_{PSM(avg)} \times (T_{3412} - T_{3324})\} \end{pmatrix} \quad (19)$$

This section has presented the proposed NB-IoT UE energy consumption model. The next sections detail the corresponding results and evaluations.

## IV. Empirical Measurements

As explained in Section I-A, works on experimental energy consumption profiling of NB-IoT radio transceivers are limited. To overcome the limitations of the state-of-the-art, a comprehensive model for profiling the empirical energy consumption of an NB-IoT radio transceiver using RRC protocol is proposed in this work. The proposed model relies on empirical measurements from two widely used CoTS NB-IoT radio boards (both equipped with BG96 module) with network configurations from two MNOs operating NB-IoT test networks at Tallinn University of Technology, that are referred to as Operator1 and Operator2.

### A. Experimental Setup

The two CoTS NB-IoT radio modules i.e., Avnet Silica NB-IoT sensor shield [27] and Quectel UMTS & LTE EVB Kit [28] that are based on 3GPP Rel-13 compliant Quectel BG96 LPWAN module [29] are used for conducting the current and power consumption measurements while in actual operation under two publicly available Operator1 and Operator 2 networks that are providing telecommunication services including NB-IoT across Estonia and other Baltic countries. A Keysight Technologies N6705C DC Power Analyzer (PA) [30] is used for collecting the current and power traces during these

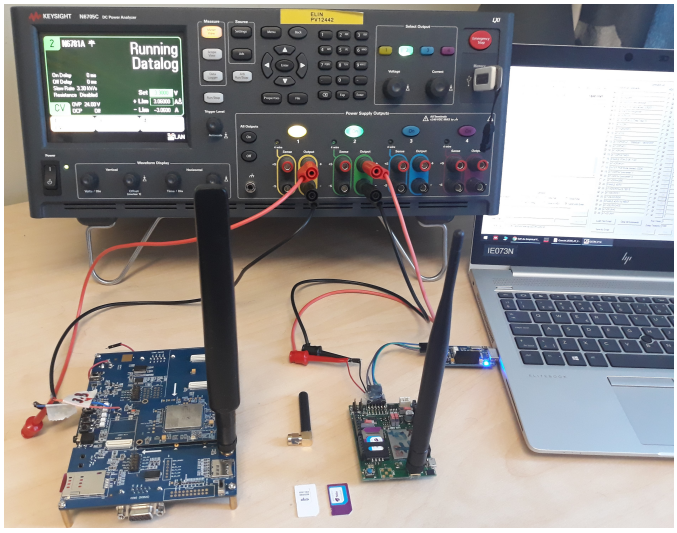


Figure 2: Testbed Setup with Quectel BG96 and Avnet Silica BG96 NB-IoT radio modules, Keysight N6705C DC Power Analyzer, and SIM cards from Operator 1 and Operator 2.

Table I: Details of the publicly available NB-IoT networks that have been used during our measurement campaigns on test location

| Details | Operator 1 | Operator 2 |
|---|---|---|
| Operator numeric code | 24801 | 24802 |
| Selected Access Technology | CAT-NB1 | CAT-NB1 |
| Selected Band | LTE BAND 20 | LTE BAND 20 |
| Selected Channel ID | 6254 | 6152 |
| CE level (at test location) | 0,1 | 0,1 |
| RSSI (average) | -72 dB | -62 dB |
| RSRP (average) | -79 dB | -72 dB |
| SINR (average) | 86 | 167 |
| RSRQ (average) | -7 dB | -9 dB |

Table II: Operator specific and UE configurable parameters

| Network Params | Symbol | Value |
|---|---|---|
| Attach | *T_ATTACH* | Network_conditions |
| Inactivity Timer | *InactivityTimer* | Operator_defined |
| C-DRX Cycle | *CDRX_Cycle* | Operator_defined |
| RRC_Idle | *RRC_Idle* | UE defined = T3412 Timer value |
| Active Timer | *T3324 Timer* | UE defined = T3324 Timer value |
| eDRX Cycle | *eDRX_Cycle* | Network defined; UE configurable |
| PagingTimeWindow | *PTW* | Network defined; UE configurable |
| eDRX_Opportuity | *eDRX_Opp* | (eDRX_Cycle - PTW) |
| I-DRX Cycle | *I-DRX_Cyc* | Operator_defined |
| PowerSavingMode | *PSM* | UE defined = (T3412-T3324) value |

measurement campaigns. Our test-bed setup with Avnet shield as our DUT1 and Quectel EVB Kit as our DUT2, along with the Keysight's PA is shown in Figure 2. A constant voltage of 3.3 volts is supplied to DUT1 and 3.8volts to DUT2 by the PA. AT commands are sent from the QCOM software running over the PC through the USB-PMOD interface for DUT1 and USB interface, configured accordingly, for DUT2. SIM cards for both the networks under test are also visible in our setup, as shown in Figure 2.

From the technical perspective, it should be mentioned here that though the BG96 module was flashed with latest firmware (FW) for both of the DUTs, setting up the (T3324/T3412) timers to our desired values was a cumbersome procedure. Upon contacting Quectel, it turned out that even the latest FW (i.e., BG96MAR02A07M1G) had its updates in the form of its sub-versions where installing the latest sub-version (i.e., BG96MAR02A07M1G_01.016.01.016) solved most of the Timers' related issues. Similarly, the built-in USB-USB interface on DUT1 that is provided to receive power and AT commands from PC, disrupted the power measurements from the PA. To avoid these disruptions, we used an FTDI chip based serial communication interface to utilize its built-in USB-UART PMOD interface [31] and bypassing its USB-USB port. We also disabled all the functional LEDs [32] of DUT1 so as to get its accurate power consumption measurements from PA. As for testing DUT2, we also modified it as per the documents provided to us by the Quectel Team. Similarly, the details of two MNOs NB-IoT test networks that have been considered for carrying out this research are summarized in Table I. Small variations in the values of RSSI, RSRP, RSRQ and SNR for the same test location could be observed from the data presented in the Table I. Table II summarizes the network parameters that are operator specific and UE configurable with a short description on their control and possible values.

### *B. Measurements Approach*

The Data Logger function of the Keysight PA records the output (voltage, current, and power) data logs of the arbitrary waveform at a sampling rate of 50 KHz. The display of the PA can be configured to examine these waveforms with a precision of upto 20 micros. For example, in Figure 3, the waveform for the power consumption of BG96 radio under real network is recorded as a data log file by the Keysight PA. This data log file is displayed in the "Maker View" of the data logger screen where the power trace P1 (Labelled as 3 in Figure 3) is displayed with 100 mW/Div (Label 1 in Figure 3) on vertical/power scale and 20.0 s/d (Lable 4 of Figure 3) on horizontal/time scale of the PA screen. The voltage (V1) and current (I1) (under Label 1 in Figure 3) are not selected for readability. The markers m1 and m2 (Label 2 in Figure 3) are set to positions where they intersect the P1 trace of the BG96 radio at the beginning and end of its C-DRX mode (Active waiting); such that the information available under label 5 to 10 presents the data available between m1 and m2 markers and can be read as summarized in Table III.

All the measurement results presented in rest of this paper are recorded as data log files and displayed in the Marker view of the PA, similar to the one as shown in Figure 3. This approach is used to produce actual power traces of the BG96 radio under real network with on-field measurements from the PA. For all the power measurements and energy calculations of rest of the waveforms/traces in this paper, Label 9 provides the average power consumption and average timings between the m1 and m2 markers; that are set at various positions on the respective power traces to obtain the concerned power consumption and timings details of the various states of the BG96 radio.

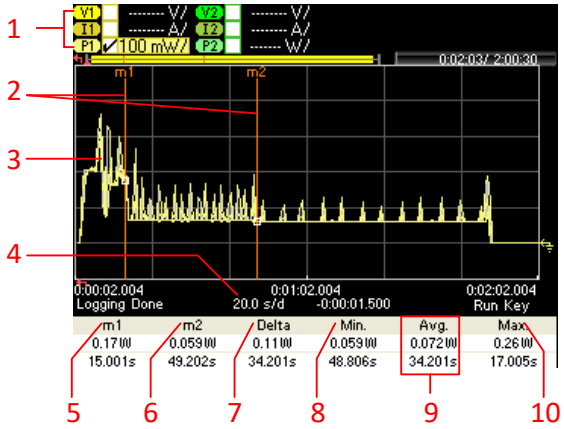


Figure 3: Measurement Setup with Keysight N6705C DC Power Analyzer: Example of an NB-IoT waveform and measurement information available in the Marker View.

Table III: Reading Data from the Marker View of the Power Analyzer

| Symbol/Field | Description |
|---|---|
| 1 Trace Controls | Identifies the voltage/div. or current/div. settings. Tick ($\surd$) indicates the trace is on. Dots ($\cdots$) indicate the trace is off. *In current setup, we only select the power trace.* |
| 2 m1/m2 markers | Shows where the measurement markers intersect the selected waveform. Data values at the bottom of the display (i.e. labelled 5-10) are referenced to the intersect locations of the markers. Calculations are based on the data points in between the intersect locations. |
| 3 Data Trace | Voltage, Current, Power trace as selected in Label 1. |
| 4 Time/Div. | Identifies the horizontal time-base setting i.e., the scale of each horizontal square on the screen. |
| 5 m1 | Indicates the m1 marker value in volts, amps, or watts at the intersection point. Also indicates the distance in time of the m1 marker in relation to the present trigger position. |
| 6 m2 | Indicates the m2 marker value in volts, amps, or watts at the intersection point. Also indicates the distance in time that the m2 marker is in relation to the present trigger position. |
| 7 Delta | Indicates the absolute difference ($\Delta$) between the markers in units (volts, amps, or watts) and in time (s). |
| 8 Min. | Indicates the minimum data value (in volts, amps, or watts) between the marker locations of the selected waveform. Also indicates the distance in time of the minimum value in relation to the present trigger position. |
| 9 Avg. | Calculates the average data value (in volts, amps, or watts) between the marker locations of the selected waveform. Time indicates the time between markers over which the average value is calculated. *For all the measurements in rest of this work, we only consider the average values of power consumption and elapsed time for the power trace in between the m1 and m2 markers that are indicated by the current 'Avg.' field.* |
| 10 Max. | Indicates the maximum data value (in volts, amps, or watts) between the marker locations of the selected waveform. Also indicates the distance in time of the maximum value in relation to the present trigger position. |

### C. Empirical Results

A number of experiments were conducted using two CoTS NB-IoT radio modules operating under two MNOs operating NB-IoT test networks in Tallinn, Estonia. To verify and evalaute the correctness of our proposed model, various timings for the different states of the NB-IoT radio modules were tried and tested for different power saving schemes. The generated results were tested for various versions of the FWs of these radio modules to verify their impact on the performance of the NB-IoT radio as they are continuously updated and to see to what extent they are compliant with the 3GPP defined NB-IoT standards. Our obtained results from these tests are explained in the subsections to follow.

*1) Testing active waiting (C-DRX) mode of the Avnet BG96 radio under Operator1 network:* To evaluate the detailed fine-grained energy consumption of the C-DRX mode of BG96 radio; we set the network parameters to C-DRX = 1, eDRX = 0 and PSM = 0 and obtained our empirical results for Operator1 network as shown in Figure 4. It could be observed that Operator1 had no limitations on the duration of its C-DRX mode as the radio remains in its active waiting state for as long as it is powered on. This is shown in Figure 4b where the average power consumption for the entire C-DRX mode is measured to be 0.082 W. Figure 4c details each C-DRX cycle of 2.56 s with an average power consumption of 0.082 W. Figure 4a details the attach procedure of the BG96 radio with Operator1 network with an average power consumption of 0.18 W over 18.6 s.

During the second phase of the same experiment, the C-DRX mode of the BG96 radio was limited to a duration of 4 m, after which the radio was forced to switch to its PSM state as shown in Figure 5. The respective average power consumption for the C-DRX mode and C-DRX cycle as shown in Figure 5a and Figure 5c were found to be the same as previously. However, the average power consumption for the PSM of BG96 radio was found to be 0.19 mW as shown in Figure 5b.

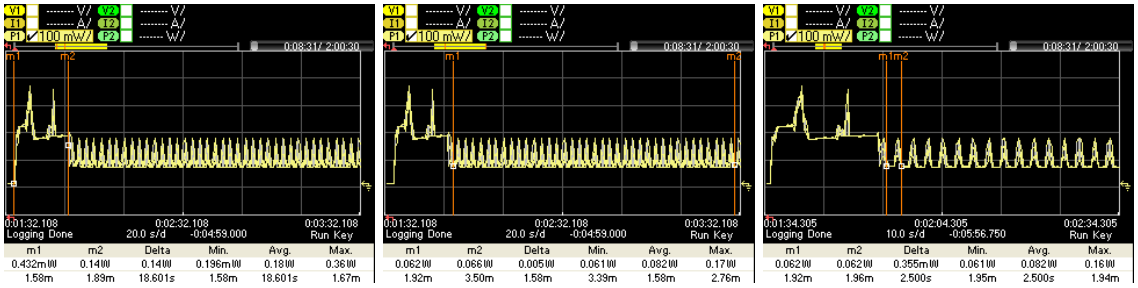

(a) Connect/Attach Mode (b) Active waiting (C-DRX Mode) (c) C-DRX Cycle

Figure 4: Continuous CDRX Mode with BG96/Avnet shield under Operator 1: (a) Power trace of UE's Attach procedure with an average power consumption of 0.18 W; (b) Power trace of C-DRX mode with an average power consumption of 0.082 W; (c) Power trace of UE's C-DRX cycle with an average power consumption of 0.082 W.

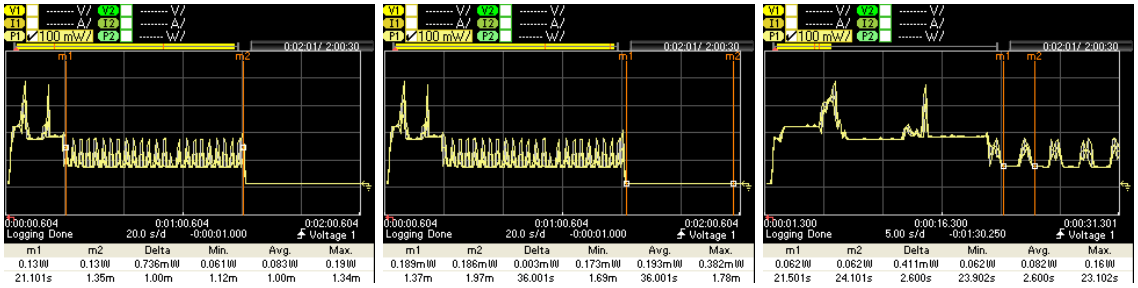

(a) C-DRX Mode (controlled) (b) PSM (c) C-DRX Cycle

Figure 5: Controlled C-DRX Mode with BG96/Avnet shield under Operator1: (a) Power trace of UE's C-DRX mode with an average power consumption of 0.083 W; (c) Power trace of UE's PSM with an average power consumption of 0.19 mW; (d) Power trace of UE's C-DRX cycle with an average power consumption of 0.082 W.

*2) Testing idle waiting (eDRX) mode of Avnet BG96 radio under Operator1 network:* To evaluate the detailed and fine-grained energy consumption of the eDRX mode of the BG96 radio with its underneath details of eDRX cycles, PTWs, and I-DRX cylces; we carried out a second series of experiments where we set the network parameters to C-DRX = 0, eDRX = 1, and PSM = 1 with T3324 timer = 4 m; such that the eDRX mode runs for 4 m and then switches to its PSM state. Our results from these experiments are summarized in Figure 6. The average power consumption for the entire eDRX mode was found to be 0.071 W as shown in Figure 6a, 0.070 W for each eDRX cycle of 41.40 s as shown in Figure 6b, and 0.078 W for the PTW of 19.80 s each as shown in Figure 6c. The I-DRX cycle is found to be 2.56s with an average power consumption of 0.081 W as shown in Figure 6d.

*3) Testing power cycle (a repeated sequence of C-DRX, eDRX, and PSM) of the Avnet BG96 radio under Operator1 network:* In these set of experiments, we evaluated the fine-grained energy consumption of the BG96 radio in a power cycle consisting of C-DRX mode, eDRX-Mode, and PSM with T3324 timer set to 4 m and T3412 set to 1 h; the results are shown in Figure 7. All the obtained results were found to be the same as Experiment 1 and Experiment 2, previously. Furthermore, it was observed that the radio automatically wakes up from its PSM to re-attach with the network and repeat its power cycle with its previous settings. The power traces for the C-DRX, eDRX and PSM states during these experiments are shown in Figures 7a, 7b, 7c.

Furthermore, we transmitted 10 bytes of data from the BG96 radio on Operator1 network using UDP protocol at different coverage levels, as shown in Figure 8a, 8b. It was observed that the radio consumed 0.000372 Wh to transmit data at CEL=0 whereas it consumed 0.000816 Wh to transmit the same data at CEL=1, i.e. an increase of 124.09% in the radio energy consumption.

*4) Testing power cycle of the Avnet BG96 radio under Operator2 network:* All the above experiments were repeated for Avnet BG96 shield under similar conditions but this time with Operator 2's network. The obtained results from these tests are summarized in Figure 9. During these tests, it was observed that Operator 2's network had more restrictions on their network parameters as compared to Operator 1 's network, i.e. the UE/radio had little provisions to configure the network parameters. For example, the C-DRX mode was fixed to 34 s (during all our tests) where the eDRX mode and PSM could be configured by the UE as desired. However, the eDRX cycle and its underneath PTW of the C-DRX mode could not be configured (contrary to the case with Operator 1). It was also noted that the radio took on an average 12.6 s to get connected to Operator 2's network, as compared to an average of 18 s with Operator 1's network.

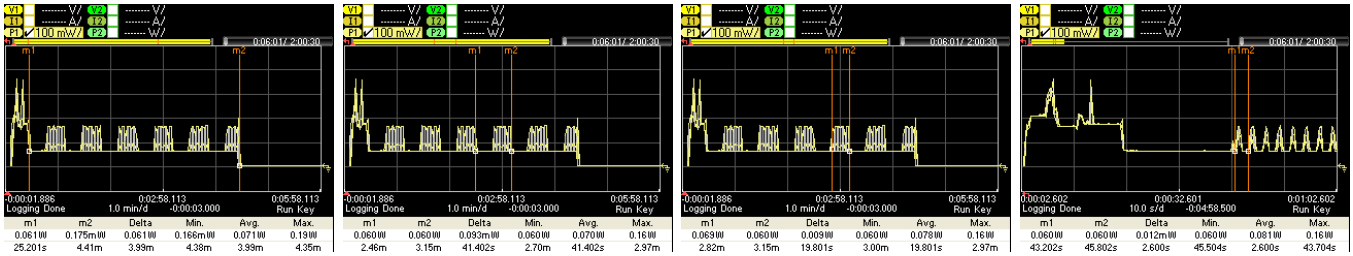

(a) eDRX Mode (b) eDRX Cycle (c) PTW (d) I-DRX Cycle

Figure 6: eDRX Mode (i.e., C-DRX = 0, PSM = 1, and T3324 = 4 m) with BG96/Avnet shield under Operator1: (a) Power trace of UE's eDRX mode with an average power consumption of 0.071 W; (b) Power trace of UE's eDRX cycle with an overall average power consumption of 0.070 W; (c) Power trace of UE's PTW with an average power consumption of 0.078 W (d) Power trace of I-eDRX cycle with an average power consumption of 0.081 W.

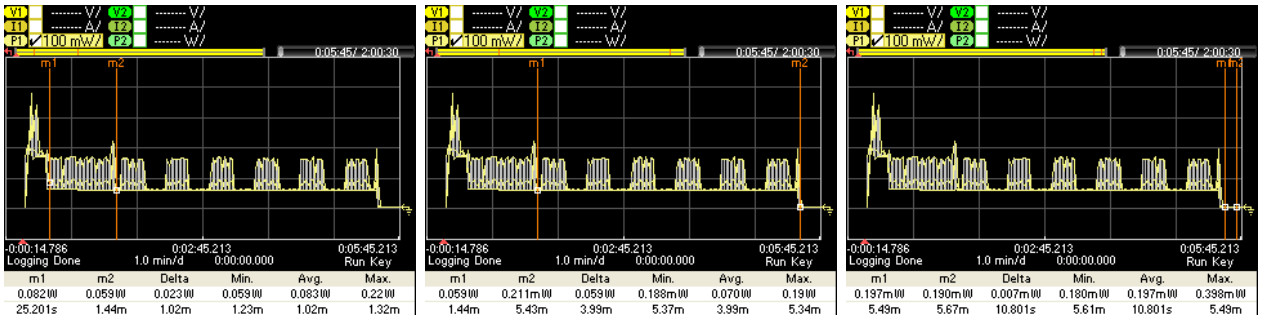

(a) C-DRX Mode (b) eDRX mode (c) PSM

Figure 7: Power cycle with BG96/Avnet shield under Operator1 network: (a) C-DRX mode runs for 1.0 m (UE configured), (b) eDRX mode runs for 4 m (UE configured), and (c) PSM runs for 60 m (UE configured), not shown in full for readability.

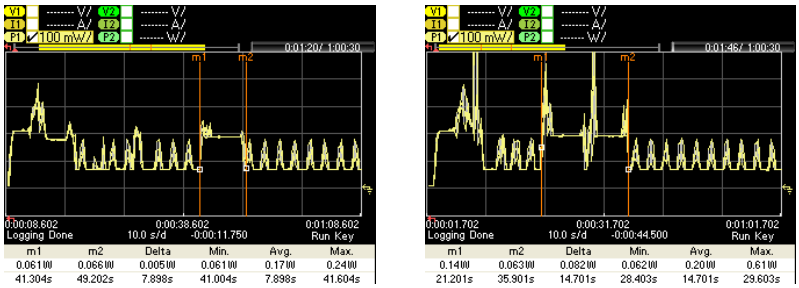

(a) Data Transmission at CEL=0 (b) Data Transmission at CEL=1

Figure 8: Transmitting 10 bytes of data using UDP protocol on Operator1 network. (a) Data Transmission at CEL=0 consumes 0.17 W for 7.898 s (0.000372 Wh), (b) Data Transmission at CEL=1 consumes 0.20 W for 14.701 s (0.000816 Wh), i.e. an increase of 119.35%.

Furthermore, we transmitted 10 bytes of data from the BG96 radio on Operator 2's network using UDP protocol at different coverage levels as shown in Figures 10a and 10b. It was observed that the radio consumed 0.00011 Wh at CEL=0 whereas it consumed 0.00016 Wh to transmit the same data at CEL=1, i.e. an increase of 45.45% in the radio energy consumption. Similarly, a comparison between the effects of overheads involved in the two data transmission protocols (i.e,. UDP and HTTPs) on the energy consumption of the radio was also made where a desired data of 10 bytes (that was required to be sent from the radio) was transmitted from the BG96 radio on Operator 2's network at different coverage levels, with additional 61 bytes of data that was the requirement of the HTTPs protocol for its server setup. The obtained power traces from these experiments are shown in Figure 11a and 11b. It was observed that the radio consumed 0.00052 Wh at CEL=0 and 0.00080 Wh at CEL=1 for the transmission of same 71 Bytes of data through HTTPS protocol; an increase of 53.8% in the energy consumption at CEL change i.e, when radio transmits with more power and for longer time. In comparison to UDP transmission protocol, this was an increase of 372% and 400% at CEL=0

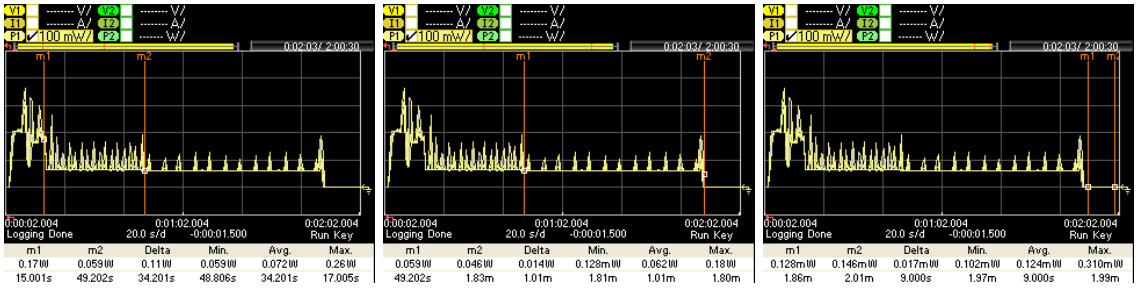

(a) C-DRX mode of 34 s. (b) eDRX mode (c) PSM

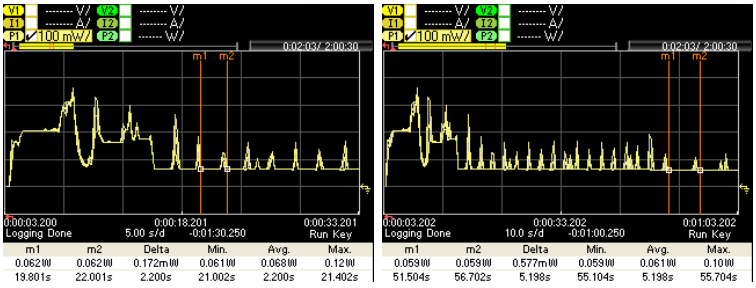

(d) C-DRX Cycle (e) I-DRX Cycle

Figure 9: Power cycle of the Avnet BG96 shield under Operator2 network: (a) C-DRX mode runs for 34.2 s, (b) eDRX mode runs for 1.0 m (UE configured), and (c) PSM runs for 1.0 h (UE configured), not shown in full for readability. In Operator 2 network, the C-DRX Cycle is 2.1 s while the I-DRX Cycle is 5.12 s.

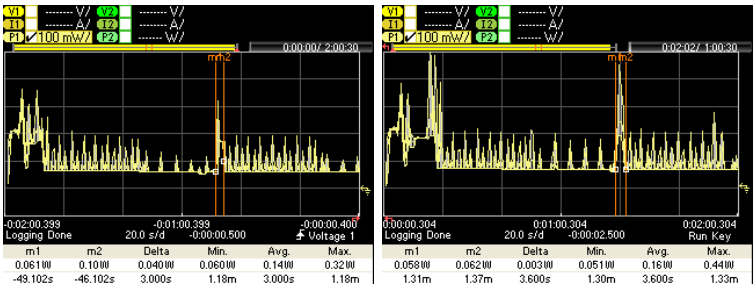

(a) Data transmission at CEL=0 (b) Data transmission at CEL=1

Figure 10: Transmitting 10 byte of data using UDP protocol on Operator2 network. (a) Data Transmission at CEL=0 consumes 0.14 W for 3 s (0.00011 Wh), (b) Data Transmission at CEL=1 consumes 0.16 W for 3.6 s (0.00016 Wh), i.e. an increase of 45.45%.

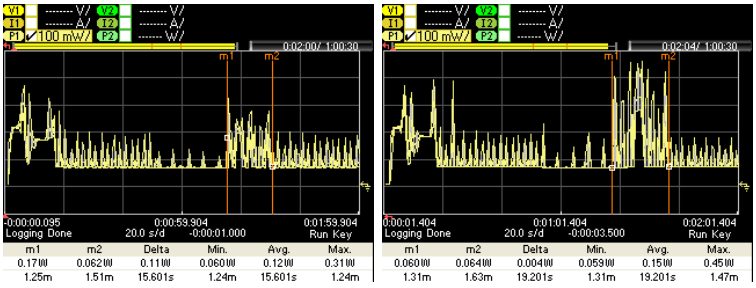

(a) Data transmission at CEL=0 (b) Data transmission at CEL=1

Figure 11: Transmitting 71 bytes of data to ThingSpeak server [33] using HTTPS protocol on Operator2 network. (a) Data Transmission at CEL=0 consumes 0.12 W for 15.6 s (0.00052 Wh), (b) Data Transmission at CEL=1 consumes 0.15 W for 19.2 s (0.0008 Wh), i.e. an increase of 53.84%.

and CEL=1, respectively, because of transmitting the extra 61 bytes of data overhead.

Tables IV and V summarize the power consumption of various states of the Avnet Silica BG96 shield under Operator1 and Operator2 test networks, respectively.

*5) Verifying our results for Operator1 and Operator2 networks with Quectel BG96 EVB Kit:* The above tests were repeated for both the operators on the same location and under similar conditions using Quectel BG96 EVB kit [28]. Since similar power graphs for C-DRX, eDRX, and PSM modes of the BG96 radio were obtained from the power analyzer, these graphs are not included in the paper for conciseness. Nevertheless, the results obtained for all these tests are summarized in Tables VI and VII.

Finally, a side by side comparison of the current and power consumption of the two boards, for both networks, are also summarized in Tables VIII and Tables IX.

### *D. Summary and discussion of the measurement results*

In the remainder of this section, we summarize our main observations of the experimental results and present a discussion thereof.

As indicated previously, Table IV summarizes the current and power consumption details of the Avnet shield under Operator1's network, whereas Table V summarizes the current and power consumption details of the Avnet board under Operator2's network. Comparing the current and power data from both of these tables, it can be noted that with Operator1's network, the BG96 radio consumes more power on average for most of its operational modes as compared to when operating on Operator2' network. It can also be noted that contrary to the other radio modes, the power and current data values for the PSM are the same with both networks[1]

The same observations stand true while comparing the current and power consumption data in Table VI and VII as obtained for the Quectel BG96 EVB kit for both of these networks. It is clear that the BG96 radio consumes more power on average for most of its operational modes when connected to Operator1's network as compared to Operator2.

However, comparing the current and power consumption data as obtained for both of these boards i.e., Avnet Silica and Quectel EVB kit, it is also clear that the latter consumes more for the same network parameters and under the same network conditions.

To have a better overview of all the data from the above-mentioned tables, we have further summarized them in Table VIII and Table IX. All in all, it can be said that from the network side Operator1 has a higher energy consumption, while from the device side, the Quectel EVB Kit consumes more.

While the current and power consumption differences between the two boards can be explained by the fact the Quectel EVB kit features more active components than the Avnet Silica board, the differences between the two networks call for a more detailed discussion, as presented in what follows.

An essential point to keep in mind is that the UE settings affect its energy consumption to a great extent, in particular in terms of active waiting, idle waiting and PSM; at the same time, these also have a notable impact on the application QoS. In parallel, the network settings also have a significant impact on the energy consumption of the UE. In more details,

i) The inactivity timer is operator specific; thus, depending on the network configuration, this can be a major energy-saving factor on the UE side. Our results have shown that Operator2 provides greater flexibility in terms of control and configurability of the C-DRX (within the inactivity timer) mode as compared to Operator1. On the other hand, Operator1 does not limit the length of its active waiting period (within the inactivity timer). This explains why Operator1 consumes more as compared to Operator 2 since the latter has a controlled active waiting period. Moreover, since the inactivity timer is reset after each downlink data exchange, the longer its span, the larger its impact on the UE energy consumption. Similarly, if downlink data is received in fragments, the impact of the energy consumption due to the inactivity timer will add-up.

ii) The activity timer is UE configurable, but its underneath eDRX cycles with its PTW and its underneath I-DRX cycles are network specific; thus, their settings affect the overall energy-consumption of the UE. Operator2 also provides greater flexibility in terms of control and configurability of its eDRX settings as compared to Operator1; since the former supports more robust settings for these parameters, it is thus more energy-friendly from the UE perspective. However, the effects of such parameters on the QoS of application is still unknown and is beyond the scope of this paper. Though Operator 1 provides more flexibility in these settings, the overall energy consumption for the radio is higher.

iii) The power consumption for PSM of the radio is nearly identical for both operators. This can be explained by the fact that when in the PSM mode, most parts of the radio module are turned off and no operator specific parameter affect the current drawn by the chip. However, a general comment is that while the longer the radio stays in PSM the larger its energy savings, this translates in increased latency cost and thus possibly reduced QoS for the application. This important trade-off in NB-IoT is not yet fully explored in the literature.

iv) Our experiments have also shown that the transmission power varies with the signal strength of the radio and thus affects the UE energy consumption. The transmit power can be ramped-up to a maximum of 23 dBm, whether when connecting to the basestation or while transmitting data. For example, in Figure 11a it can be seen that the power for data transmission is 0.12 W (i.e., 20.79 dBm) and 0.15 W (i.e., 21.76 dBm) in Figure 11b. Since the UE has no provision

[1]It is also noted that the average current consumption for PSM = 0.05 mA, which is higher than the 0.01 mA value indicated in the datasheet [29]. Such difference can be due to the additional components needed to implement a BG96 minimum system on the Avnet shield (e.g. power regulator, USB interface, etc.). Such difference is also in line with our observation that, in a practical system, the energy consumption of NB-IoT radio transceivers is often under-estimated.

Table IV: Summary of the power consumption of various states of the Avnet Silica BG96 shield under Operator1 network

| **Avnet Silica BG96 shield current and power consumption details with a constant 3.3V power supply** | | |
|---|---|---|
| **Operational Modes** | ***Avg Current*** | ***Avg Power*** |
| **Attach/Resume Procedure ( ≈ 18s)** | **56.8 mA** | **180 mW** |
| **C-DRX Mode(Not fixed to any value)** | **25.1 mA** | **82 mW** |
| C-DRX Cycle = 2.56 s | 25.1 mA | 82 mW |
| On duration (PO) = 1.28 s | 32 mA | 110 mW |
| Off duration (SP) = 1.28 s | 18.1 mA | 59 mW |
| **eDRX Mode (as defined by T3324 = 4 m)** | **21.8 mA** | **71 mW** |
| eDRX Cycle= 40.96 s | 21.8 mA | 70 mW |
| PTW = 20.48 s | 25.5 mA | 78 mW |
| I-eDRX Cycle = 2.56 s | 24.47 mA | 81 mW |
| On duration (PO) = 1.28 s | 31 mA | 110 mW |
| Off duration (SP) = 1.28 s | 17.98 mA | 59 mW |
| eDRX Opportunity = 20.48 s | 17.97 mA | 59 mW |
| **PSM Mode (as defined by (T3412-T3324) value)** | **0.05 mA** | **0.19 mW** |

Table V: Summary of the power consumption of various states of the Avnet Silica BG96 shield under Operator2 network

| **Avnet Silica BG96 shield current and power consumption details with a constant 3.3V power supply** | | |
|---|---|---|
| **Operational Modes** | ***Avg Current*** | ***Avg Power*** |
| **Attach/Resume Procedure ( ≈ 12 s)** | **40.1 mA** | **190 mW** |
| **C-DRX Mode (Fixed to 34 s)** | **21.3 mA** | **72 mW** |
| C-DRX Cycle = 2.1 s | 21.2 mA | 70 mW |
| On duration (PO) = 0.5 s | 28 mA | 98 mW |
| Off duration (SP) = 1.6 s | 18.6 mA | 62 mW |
| **eDRX Mode (as defined by T3324)** | **19.2 mA** | **63 mW** |
| eDRX Cycle = 5.12 s (Fixed) | 18.8 mA | 62 mW |
| On duration (PO) = 0.3 s | 26.2 mA | 87 mW |
| Off duration (SP) = 4.7 s | 18.2 mA | 60 mW |
| **PSM Mode (as defined by (T3412-T3324) value)** | **0.03 mA** | **0.12 mW** |

Table VI: Summary of the power consumption of various states of QUECTEL BG96 EVB Kit under Operator1 network

| **QUECTEL BG96 Kit current and power consumption details with a constant 3.8V power supply** | | |
|---|---|---|
| **Operational Modes** | ***Avg Current*** | ***Avg Power*** |
| **Attach/Resume Procedure ( ≈ 18 s)** | **51.8 mA** | **200 mW** |
| **C-DRX Mode(Not fixed by the operator)** | **26.1 mA** | **100 mW** |
| C-DRX Cycle = 2.56 s | 25.6 mA | 97 mW |
| On duration (PO) = 1.28 s | 30.6 mA | 120 mW |
| Off duration (SP) = 1.28 s | 20.1 mA | 78 mW |
| **eDRX Mode (as defined by T3324 = 4 m)** | **20.22 mA** | **77 mW** |
| eDRX Cycle= 40.96 s | 20.22 mA | 77 mW |
| PTW = 20.48 s | 22.77 mA | 87 mW |
| I-eDRX Cycle = 2.56 s | 22.57 mA | 86 mW |
| On duration (PO) = 1.28 s | 27.6 mA | 100 mW |
| Off duration (SP) = 1.28 s | 16.9 mA | 66 mW |
| eDRX Opportunity = 20.48 s | 17.1 mA | 66 mW |
| **PSM Mode (value of (T3412-T3324))** | **0.05 mA** | **0.20 mW** |

Table VII: Summary of the power consumption of various states of QUECTEL BG96 EVB Kit under Operator2 network.

| **QUECTEL BG96 kit current and power consumption details with a constant 3.8V power supply** | | |
|---|---|---|
| **Operational Modes** | ***Avg Current*** | ***Avg Power*** |
| **Attach/Resume Procedure ( ≈ 12s)** | **59.3 mA** | **190 mW** |
| **C-DRX Mode (Fixed to 34 s)** | **25.3 mA** | **86 mW** |
| C-DRX Cycle = 2.1 s | 25.2 mA | 85 mW |
| On duration (PO) = 0.5 s | 28 mA | 170 mW |
| Off duration (SP) = 1.6 s | 18.6 mA | 78 mW |
| **eDRX Mode (as defined by T3324)** | **19.2 mA** | **63 mW** |
| eDRX Cycle = 5.12 s (Fixed) | 30.8 mA | 100 mW |
| On duration (PO) = 0.4 s | 29.8 mA | 98 mW |
| Off duration (SP) = 4.7 s | 22.9 mA | 76 mW |
| **PSM Mode (value of (T3412-T3324))** | **0.05 mA** | **0.19 mW** |

to control its transmit power, the energy consumption from the UE transmit power point of view is not an exclusive UE feature.

v) The data transmission protocol varies in terms of their control overheads, data payloads, coverage level, and security/guarantees. These various protocols consume different energy consumption as seen in our experimental results when transmitting data with the UDP and HTTPs protocols in two

Table VIII: Side by side comparison of the average power measurements of Avnet BG96 shield and Quectel BG96 EVB Kit under Operator1 and Operator2 networks

| **Power Consumption of the Avnet BG96 shield and Quectel BG96 EVB Kit** | | | | |
|---|---|---|---|---|
| Quectel / Avnet | **Attach (mW)** | **CDRX (mW)** | **eDRX (mW)** | **PSM (mW)** |
| **Operator 1** | 200 / 180.0 | 100 / 82.0 | 77.0 / 71.0 | 0.20 / 0.19 |
| **Operator 2** | 190 / 190.0 | 86.0 / 72.0 | 63.0 / 63.0 | 0.19 / 0.12 |

Table IX: Side by side comparison of the average current measurements of Avnet BG96 shield and Quectel BG96 EVB Kit under Operator1 and Operator2 networks

| **Current consumption of the Avnet BG96 shield and Quectel BG96 EVB Kit** | | | | |
|---|---|---|---|---|
| Quectel / Avnet | **Attach (mA)** | **CDRX (mA)** | **eDRX (mA)** | **PSM (mA)** |
| **Operator 1** | 51.8 / 56.8 | 26.1 / 25.1 | 20.22 / 21.8 | 0.05 / 0.05 |
| **Operator 2** | 59.3 / 40.1 | 25.3 / 21.3 | 19.2 / 19.2 | 0.05 / 0.03 |

different coverage classes. For example, Figures 8, 10 show that transiting from coverage level CEL=0 to CEL=1 with UDP leads to energy consumption increases between 45% and 119%, i.e. up to more than a factor 2. Figure 11a and Figure 11b show the same transition with HTTPs leads to an increase of 53.84%, i.e. slightly more than a factor 1.5. Also, as mentioned earlier, the increase between UDS and HTTPs ranges from 372% and 400%.

Moreover, from the results obtained through these experiments, it is clear that almost all of the 3GPP defined UE states are attainable on MNO's test networks, and thus by extension on commercial networks; this is in stark contrast to what has been reported in most of the existing literature so far. The results also indicates that all the power saving features of the NB-IoT technology are included in the considered CoTS NB-IoT radio chips and could be utilized as per the application requirements. However, as the hardware and software developments of NB-IoT are ongoing, special care must be taken to choose the right firmware for the right hardware that is being used for the specific application. Our results also show that all the timers are flexible and can be set as per the 3GPP standard provided the network operators allow any such provisions from the network side and this should be kept in mind by any application developer to obtain network access.

## V. Evaluation of our Proposed Model

Section IV has presented individual empirical measurement results for various timings for the different states of the NB-IoT radio module for different power saving schemes. Next, in this section we evaluate the proposed model by calculating the difference between the energy consumption obtained from the real life deployment versus that predicted by the model. We have conducted three sets of experiments of which the base cycle lasts from 12.3 m to 1.2 h and is repeated from 2 to 10 times during the observation window. Doing so puts the NB-IoT radio in various operational conditions and allows characterizing the average differences between the energy consumption predicted by the model and the real-life values. The three sets of experiments use the Avnet BG96 shield operating on Operator1 or Operator2 network, as described in what follows.

The first evaluation test was executed with an Avnet BG96 shield board operating on Operator1 network. The test consisted of a base power cycle of 30 m as captured between m1 and m2 (29.55 m shown) in Figure 12a and repeated twice in an observation window of 1 h (59.53 m shown) between m1 and m2 as show in Figure 12b. As can be seen in Figure 12a, the base power cycle includes an attach procedure of 18 s, and C-DRX, e-DRX and PSM states of a bit less than 10 m each where the average power consumption for the base power cycle is 0.052 W. And as can be seen in Figure 12b, it is repeated twice over a period of 60 m as shown between m1 and m2 (59.53 m shown) where the average power consumption is found to be 0.052 W. The energy consumed per each power cycle as per Equation (19) is 0.022 Wh, whereas that measured with the PA is 0.026 Wh. The energy consumed for the entire observation window as per Equation (19) is 0.044 Wh, whereas that measured with the PA is 0.052 Wh, i.e. an error of 15.38%, as indicated in Table X.

The second evaluation test also used an Avnet BG96 shield, but this time operating on Operator2 network. The test consisted of the base power cycle as shown in Figure 13a (m1 and m2 in this figure are used to record the repeated C-DRX cycle of the radio after a data transmission (Tx)) and this power cycle is repeated 3 times as shown in Figure 13b. The base power cycle lasts 12.3 m that includes an Attach procedure of 12.1 s, C-DRX mode of 20 s, Tx through UDP protocol of 3 s, repeated C-DRX of 32 s, eDRX of 34 s, and PSM of a bit more than 10 m. The base power cycle consumes on average 0.011 W during the 12.3 m duration, i.e. an average energy consumption of 0.0022 Wh. As indicated in Table X, the energy consumed per power

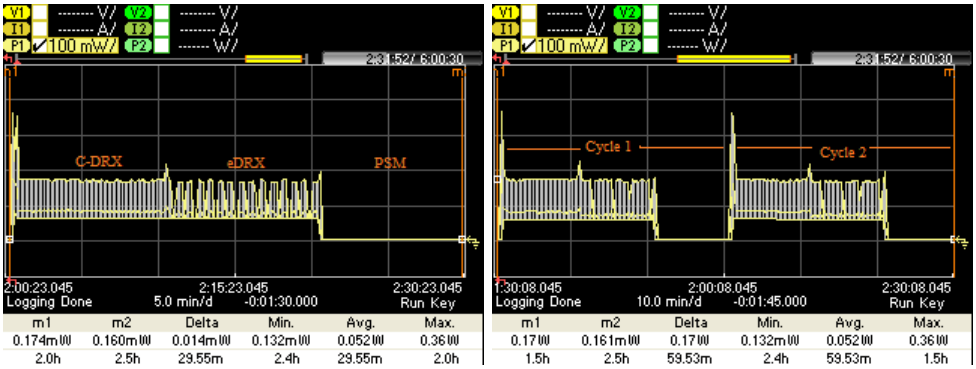


(a) A power cycle of 30 m ("29.55m" displayed between m1 and m2 markers) that includes an Attach procedure of 18 s, C-DRX, e-DRX and PSM of a bit less than 10 m each.

(b) The power cycle of (a) is repeated for 2 times in an observation window of 60 m ("59.53m" displayed between m1 and m2 markers).

Figure 12: Power traces of the first evaluation test with the Avnet BG96 shield operating on Operator1 network.

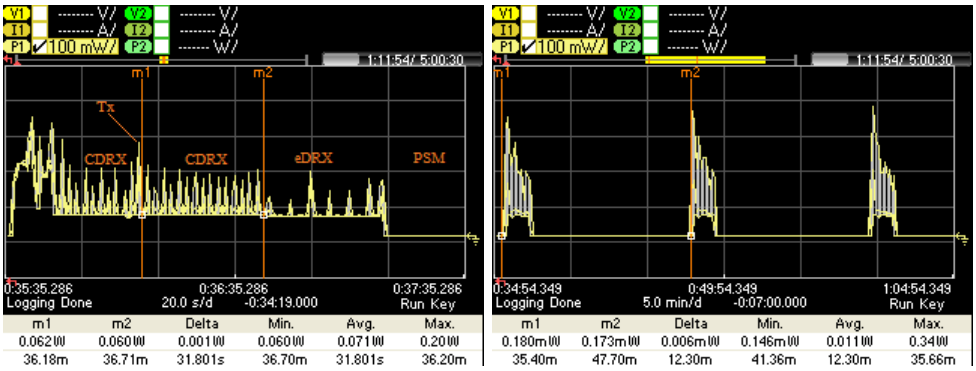


(a) A power cycle of 12.3 m that includes an Attach procedure of 12.1 s, C-DRX mode of 20 s, Tx (10 bytes data over UDP) of 3 s, repeated C-DRX of 32 s ("31.801s" displayed between m1 and m2 markers), eDRX of 34 s and PSM of a bit more than 10 m (not shown in full for readability).

(b) The power cycle of (a) 12.3 m ("12.30m" displayed between m1 and m2 markers) is repeated 3 times (The last PSM phase is not shown in full for readability)).

Figure 13: Power traces of the second evaluation test with Avnet BG96 shield on Operator2 network

cycle as per Equation (19) is 0.0024 Wh, i.e. an error of 9.09%.

Like the second one, the third evaluation test was conducted with the Avnet BG96 shield operating under Operator2 network, but his time for a longer duration. The base cycle lasts 1.2 h including an Attach procedure of 12 s, CDRX of 32 s, e-DRX of 10 m and PSM of 64 m, as shown in Figure 14a. This power cycle of 1.2 h has an average power consumption of 0.010 W. It is then repeated 10 times in an observation window of 11.8 h, as shown in Figure 14b (note that some of the PSM durations are shorter than others). In this case, the energy consumed per power cycle measured with the PA is 0.01200 Wh, whereas as indicated in Table X, as per Equation (19) it is found to be 0.01204 Wh, i.e. an error of 0.33% only.

To summarize, given the above evaluation tests, the error of the proposed model ranges from as low as 0.33% for large time spans up to ca. 15.38% for shorter time spans.

## VI. Conclusion and Future Directions

NB-IoT is an emerging technology which is expected to dominate the IoT landscape in terms of wireless communication technology for massive machine type communication. Understanding the energy budget of NB-IoT is important; however, this is weakly addressed in the state of the art. The motivation of this work is to provide a modelling methodology for profiling the baseline energy consumption of an NB-IoT radio transceiver based on the RRC protocol standardized by 3GPP. The proposed energy consumption model provides a detailed and realistic NB-IoT radio transceiver energy consumption model; the detailed analysis of the RRC protocol, empirical measurements shows detailed energy consumption of the RRC protocol for two development boards and on two MNOs test networks. Finally, real-life empirical evaluation results show that the error of the proposed model ranges

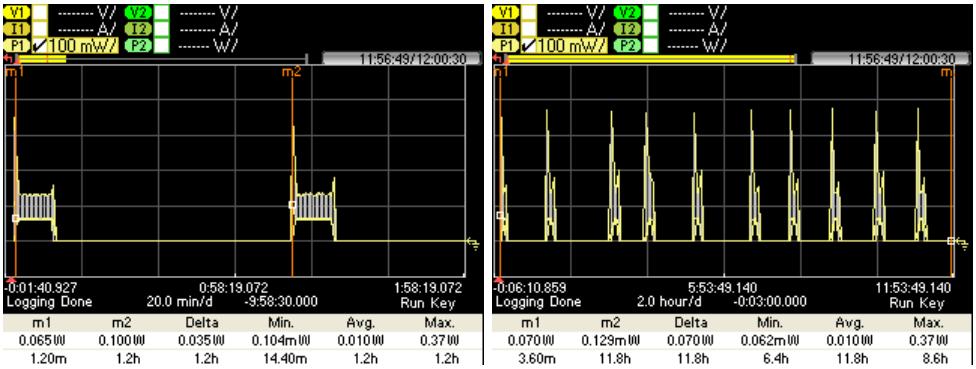


(a) A power cycle of 1.2 h ("1.2h" between m1 and m2 markers) including an Attach procedure of 12.1 s, C-DRX of 32 s, e-DRX of 10 m and PSM of 64 m.

(b) The power cycle of (a) is repeated 10 times in an observation window of 11.8 h ("11.8h" between m1 and m2 markers). (Note that some of the PSM durations are shorter than others).

Figure 14: Power traces of the third evaluation test with Avnet BG96 shield under Operator2 network.

Table X: NB-IoT radio energy consumption error: proposed model vs. real-life evaluation tests

| Test setup | Energy as per model (Wh) | Energy as per measurement (Wh) | Relative Error (%) |
|---|---|---|---|
| Avnet BG96 shield, Operator1 | 0.052 | 0.044 | 15.38 |
| Avnet BG96 shield, Operator2 | 0.0024 | 0.0022 | 9.09 |
| Avnet BG96 shield, Operator2 | 0.01204 | 0.01200 | 0.33 |

between 0.33% and 15.38%. The proposed model and its evaluation ensures that it is viable to be used as a reference benchmark for NB-IoT radio communication. In the future, the proposed baseline energy consumption model would be optimized depending upon the lifetime requirements of the given application.

## VII. ACKNOWLEDGMENT

This project has received funding partly from the European Union's Horizon 2020 Research and Innovation Program under Grant 668995 and partly from the European Union Regional Development Fund in the framework of the Tallinn University of Technology Development Program 2016–2022, and partly from Estonian Research Council grant PRG667.

## REFERENCES

[1] A. Rico-Alvarino, M. Vajapeyam, H. Xu, X. Wang, Y. Blankenship, J. Bergman, T. Tirronen, and E. Yavuz, "An overview of 3gpp enhancements on machine to machine communications," *IEEE Communications Magazine*, vol. 54, no. 6, pp. 14–21, 2016.

[2] Y.-P. E. Wang, X. Lin, A. Adhikary, A. Grovlen, Y. Sui, Y. Blankenship, J. Bergman, and H. S. Razaghi, "A primer on 3gpp narrowband internet of things," *IEEE Communications Magazine*, vol. 55, no. 3, pp. 117–123, 2017.

[3] E. U. T. R. Access, "Medium access control (mac) protocol specification (release 8)", 3gpp ts 36.321," *V8. 0.0,(Dec. 2007)*, 2008.

[4] G. T. 36.331, "Evolved universal terrestrial radio access (e-utra); radio resource control (rrc); protocol specification (release 10)," 2012.

[5] E. U. T. R. Access, "Radio resource control (rrc), 3gpp ts 36.331," 2012.

[6] C.-W. Chang and J.-C. Chen, "Adjustable extended discontinuous reception cycle for idle-state users in lte-a," *IEEE Communications Letters*, vol. 20, no. 11, pp. 2288–2291, 2016.

[7] A. K. Sultania, C. Delgado, and J. Famaey, "Implementation of nb-iot power saving schemes in ns-3," in *Proceedings of the Workshop on Next-Generation Wireless with ns-3*, 2019, pp. 5–8.

[8] A. K. Sultania, P. Zand, C. Blondia, and J. Famaey, "Energy modeling and evaluation of nb-iot with psm and edrx," in *IEEE Globecom Workshops (GC Wkshps)*. IEEE, 2018, pp. 1–7.

[9] G. Tsoukaneri, F. Garcia, and M. K. Marina, "Narrowband iot device energy consumption characterization and optimizations." in *EWSN*, 2020, pp. 1–12.

[10] C. Y. Yeoh, A. bin Man, Q. M. Ashraf, and A. K. Samingan, "Experimental assessment of battery lifetime for commercial off-the-shelf nb-iot module," in *2018 20th International Conference on Advanced Communication Technology (ICACT)*. IEEE, 2018, pp. 223–228.

[11] P. Andres-Maldonado, P. Ameigeiras, J. Prados-Garzon, J. Navarro-Ortiz, and J. M. Lopez-Soler, "Narrowband iot data transmission procedures for massive machine-type communications," *IEEE Network*, vol. 31, no. 6, pp. 8–15, 2017.

[12] P. Andres-Maldonado, M. Lauridsen, P. Ameigeiras, and J. M. Lopez-Soler, "Analytical modeling and experimental validation of nb-iot device energy consumption," *IEEE Internet of Things Journal*, vol. 6, no. 3, pp. 5691–5701, 2019.

[13] P. Andres-Maldonado, P. Ameigeiras, J. Prados-Garzon, J. J. Ramos-Munoz, and J. M. Lopez-Soler, "Optimized lte data transmission procedures for iot: Device side energy consumption analysis," in *2017 IEEE International Conference on Communications Workshops (ICC Workshops)*. IEEE, 2017, pp. 540–545.

[14] M. El Soussi, P. Zand, F. Pasveer, and G. Dolmans, "Evaluating the performance of emtc and nb-iot for smart city applications," in *2018 IEEE International Conference on Communications (ICC)*. IEEE, 2018, pp. 1–7.

[15] R. Mozny, P. Masek, M. Stusek, K. Zeman, A. Ometov, and J. Hosek, "On the performance of narrow-band internet of things (nb-iot) for delay-tolerant services," in *2019 42nd International Conference on Telecommunications and Signal Processing (TSP)*. IEEE, 2019, pp. 637–642.

[16] S. S. Basu, A. K. Sultania, J. Famaey, and J. Hoebeke, "Experimental performance evaluation of nb-iot," in *2019 International Conference on Wireless and Mobile Computing, Networking and Communications (WiMob)*. IEEE, 2019, pp. 1–6.

[17] B. Martinez, F. Adelantado, A. Bartoli, and X. Vilajosana, "Exploring the performance boundaries of nb-iot," *IEEE Internet of Things Journal*, vol. 6, no. 3, pp. 5702–5712, 2019.

[18] S. Duhovnikov, A. Baltaci, D. Gera, and D. A. Schupke, "Power consumption analysis of nb-iot technology for low-power aircraft appli-

cations," in *2019 IEEE 5th World Forum on Internet of Things (WF-IoT)*. IEEE, 2019, pp. 719–723.

[19] M. Lauridsen, R. Krigslund, M. Rohr, and G. Madueno, "An empirical nb-iot power consumption model for battery lifetime estimation," in *2018 IEEE 87th Vehicular Technology Conference (VTC Spring)*. IEEE, 2018, pp. 1–5.

[20] P. Jörke, R. Falkenberg, and C. Wietfeld, "Power consumption analysis of nb-iot and emtc in challenging smart city environments," in *2018 IEEE Globecom Workshops (GC Wkshps)*. IEEE, 2018, pp. 1–6.

[21] K. Mikhaylov, M. Stusek, P. Masek, V. Petrov, J. Petajajarvi, S. Andreev, J. Pokorny, J. Hosek, A. Pouttu, and Y. Koucheryavy, "Multi-rat lpwan in smart cities: Trial of lorawan and nb-iot integration," in *2018 IEEE International Conference on Communications (ICC)*. IEEE, 2018, pp. 1–6.

[22] M. Lukic, S. Sobot, I. Mezei, D. Danilovic, and D. Vukobratovic, "In-depth real-world evaluation of nb-iot module energy consumption," *arXiv preprint arXiv:2005.13648*, 2020.

[23] G. T. 23.401, "3GPP TS 23.401, GPRS Enhancements for Evolved Universal Terrestrial Radio Access Network (E-UTRAN) Access," 2013.

[24] ——, "3GPP, "TS 23.401 GPRS enhancements for Evolved Universal Terrestrial Radio Access Network access," Rel 14 v14.1.0, 2016," 2016.

[25] ——, "3GPP, "TS 23.401 GPRS enhancements for Evolved Universal Terrestrial Radio Access Network access," Rel 16 V16.6.0 (2020-03)," 2020.

[26] T. ETSI, "123 401 v14. 3.0," 2017.

[27] Avnet:Silica, "Avnet: Quality Electronic Components Services." [Online]. Available: https://www.avnet.com/wps/portal/silica/products/new-products/npi/2018/avnet-nb-iot-shield-sensor/

[28] Quectel UMTS LTE EVB Kit, "Quectel." [Online]. Available: https://www.quectel.com/product/umtsevb.htm

[29] Quectel LPWA IoT Module, "BG96 LTE Cat M1/NB1/EGPRS Module." [Online]. Available: https://www.quectel.com/product/bg96.htm

[30] Keysight Technologies, "N6705C DC Power Analyzer." [Online]. Available: https://www.keysight.com/en/pd-2747858-pn-N6705C/dc-power-analyzer-modular-600-w-4-slots?cc=EElc=eng

[31] Digilent, "pmod-usb-to-uart-interface." [Online]. Available: https://store.digilentinc.com/pmod-usbuart-usb-to-uart-interface/

[32] Avnet-Silica-team, "NBIOTBG96SHIELD-HW-schematic." [Online]. Available: https://github.com/Avnet-Silica-team/NBIoTBG96-HW/blob/master/BAENBIOTBG96SHIELD$_{R}SR1157C-SCHEMA.pdf$/

[33] ThingSpeak Server, "ThingSpeak for IoT Projects ." [Online]. Available: https://thingspeak.com/channels/1085017/